Cell Surface β1,4-Galactosyltransferase Functions during Neural Crest Cell Migration and Neurulation In Vivo

Helen J. Hathaway and Barry D. Shur

Department of Biochemistry and Molecular Biology, The University of Texas M. D. Anderson Cancer Center, Houston, Texas 77030

Abstract. Mesenchymal cell migration and neurite outgrowth are mediated in part by binding of cell surface β1,4-galactosyltransferase (GalTase) to N-linked oligosaccharides within the E8 domain of laminin. In this study, we determined whether cell surface GalTase functions during neural crest cell migration and neural development in vivo using antibodies raised against affinity-purified chicken serum GalTase. The antibodies specifically recognized two embryonic proteins of 77 and 67 kD, both of which express GalTase activity. The antibodies also immunoprecipitated and inhibited chick embryo GalTase activity, and inhibited neural crest cell migration on laminin matrices in vitro. Anti-GalTase antibodies were microinjected into the head mesenchyme of stage 7–9 chick embryos or cranial to Henson's node of stage 6 embryos. Anti-avian GalTase IgG decreased cranial neural crest cell migration on the injected side but did not cross the embryonic midline and did not affect neural crest cell migration on the uninjected side. Anti-avian GalTase Fab crossed the embryonic midline and perturbed cranial neural crest cell migration throughout the head. Neural fold elevation and neural tube closure were also disrupted by Fab fragments. Cell surface GalTase was localized to migrating neural crest cells and to the basal surfaces of neural epithelia by indirect immunofluorescence, whereas GalTase was undetectable on neural crest cells prior to migration. These results suggest that, during early embryogenesis, cell surface GalTase participates during neural crest cell migration, perhaps by interacting with laminin, a major component of the basal lamina. Cell surface GalTase also appears to play a role in neural tube formation, possibly by mediating neural epithelial adhesion to the underlying basal lamina.

THE mechanisms by which cells recognize and interact with their environment, either with the extracellular matrix or with neighboring cells, are initiated at the cell surface. Several cell surface receptors that function during cellular interactions have been identified, characterized, and subsequently been shown to play a critical role in embryonic development by mediating cellular adhesion or migration, or by transducing appropriate receptor-mediated signals that dictate an inductive response (Austin and Kimble, 1987; Takeichi, 1988; Drake and Little, 1991; Flanagan et al., 1991; Kramer et al., 1991; Olson et al., 1991).

One of these cell surface receptors is β1,4-galactosyltransferase (GalTase),[1] which participates in a number of cellular interactions, including cell migration and spreading on laminin matrices (Runyan et al., 1986, 1988; Eckstein and Shur, 1989; Romagnano and Babiarz, 1990), neurite initiation and outgrowth (Begovac and Shur, 1990; Begovac et al., 1991), sperm–egg binding (Lopez et al., 1985; Miller et al., 1992), embryonic cell–cell adhesion (Bayna et al., 1988; Hathaway et al., 1989), and uterine epithelial cell–cell adhesion (Dutt et al., 1987). GalTase functions as an adhesion molecule by binding to specific oligosaccharide residues in the extracellular matrix or on adjacent cells. At present it is unclear whether cell surface GalTase functions as a lectin, similar to the selectin class of carbohydrate-binding receptors (Larsen et al., 1990; Lowe et al., 1990), or catalytically, as occurs in the Golgi during glycoprotein biosynthesis. Nevertheless, with the increasing body of evidence implicating a role for carbohydrates in normal cellular processes (Kunemund et al., 1988; Reddy et al., 1989; Shur, 1989; Griffith and Wiley, 1990; Larsen et al., 1990; Lowe et al., 1990; Woo et al., 1990; Stamenkovic et al., 1991), it is important to determine the function of cell surface carbohydrate-binding glycoproteins during embryonic development.

The function of cell surface GalTase during cell migration has been studied extensively in vitro. GalTase is preferentially localized to the leading edges of migrating cells (Eckstein and Shur, 1989), where it mediates cell spreading and migration by binding to N-linked oligosaccharides within the E8 domain of laminin (Begovac and Shur, 1990). GalTase does not appear to function during initial cell adhesion to laminin (Runyan et al., 1988; Romagnano and Babiarz, 1990), nor during cell migration on matrices not containing laminin (Runyan et al., 1986; Eckstein and Shur, 1989; Romagnano and Babiarz, 1990). These processes rely upon other matrix receptors, notably the integrins (Hynes, 1987).

Correspondence may be addressed to Barry D. Shur.

1. *Abbreviation used in this paper*: GalTase, β1,4-galactosyltransferase.

Laminin induces GalTase expression onto the growing lamellipodium (Eckstein and Shur, 1989; Romagnano and Babiarz, 1990), where it becomes associated with the cytoskeleton (Eckstein and Shur, 1992), thus facilitating cell spreading and migration.

Ultimately, it is critical to determine if molecular models for cell/matrix interactions developed in vitro actually function during embryogenesis in vivo. The microinjection of mRNA into amphibian embryos (Harvey and Melton, 1988; Ruiz i Altaba and Melton, 1989) or of antibodies and competing peptides into amphibian or avian embryos (Boucat et al., 1984; Bronner-Fraser, 1985; Bronner-Fraser and Lallier, 1988) has become a useful method for identifying molecules that play a role in embryogenesis. Antibodies against specific cell surface receptors, or peptides that compete for binding to these receptors, block neural crest cell migration when injected into developing chick embryos. These results have demonstrated an in vivo role for such cell surface and extracellular matrix components as integrin (Bronner-Fraser, 1985), fibronectin (Boucat et al., 1984), the HNK-1 epitope (Bronner-Fraser, 1987), and a laminin/heparin sulfate proteoglycan complex (Bronner-Fraser and Lallier, 1988).

In this study, we examined the role of cell surface GalTase during avian embryogenesis. Anti-GalTase IgG and Fab fragments, which specifically recognized chick embryo GalTase and inhibited GalTase activity, perturbed avian neural crest cell migration on laminin matrices in vitro. When these antibodies were injected into the head mesenchyme of early chicken embryos, neural crest cell migration was inhibited. Anti-GalTase Fab fragments also induced neural tube defects due to their ability to cross the embryonic midline. GalTase was localized by indirect immunofluorescence to migrating neural crest cells, as well as to the basolateral regions of neural epithelial cells. These results suggest a role for cell surface GalTase in mediating neural crest cell migration and neurulation in vivo.

Materials and Methods

Embryos

Fertile White Leghorn chicken eggs were purchased from the Poultry Department, Texas A&M University (College Station, TX). Eggs were incubated at 38°C in a humidified chamber for 24–72 h and staged according to Hamburger and Hamilton (1951). To collect embryos for in vitro migration assays and for antibody studies, eggs were broken into sterile 0.9% saline. Embryos were removed from the yolk by cutting through the vitelline membrane, and the blastoderm was then transferred to PBS. For in vivo assays, the eggs were candled to locate the blastoderm and windowed to expose the embryo. Sterile saline was added to raise the embryo; India ink, diluted 1:4, was injected under the blastoderm to aid in visualization of the embryo. After microinjection, eggs were sealed with electrical tape, rotated 180°, and returned to a 38°C incubation chamber.

Anti-Avian GalTase Antibodies

Polyclonal anti-chicken serum GalTase antibodies have been previously characterized (Hathaway et al., 1991). Briefly, GalTase was purified from chicken serum to apparent homogeneity by α-lactalbumin affinity chromatography followed by preparative gel electrophoresis (Hathaway et al., 1991). The purified protein was used as immunogen to raise rabbit polyclonal antibodies. Antisera with titers of ≥1/160,000 were used in subsequent assays. Purified anti-GalTase IgG immunoprecipitates GalTase activity from chicken serum and from solubilized chick embryo fibroblasts, recognizes chicken serum GalTase on Western immunoblots, and inhibits chicken serum GalTase activity (Hathaway et al., 1991). IgG was prepared by protein A affinity chromatography (Goding, 1978), and Fab was prepared from purified IgG as described (Hathaway et al., 1991).

Western Immunoblotting

One hundred stage 7–12 chicken embryos were collected as described above, and the area opaca and area pellucida were removed. Embryos were rinsed twice in medium B (NaCl, 7.5 g/liter; KCl, 0.4 g/liter; Hepes buffer, 4.76 g/liter; pH 7.2), pelleted, and resuspended in 1 ml of medium B containing a protease inhibitor cocktail (2 μg/ml antipain, 0.1% aprotinin, 10 μg/ml benzamidine, 1 μg/ml chymostatin, 1 μg/ml leupeptin, and 1 μg/ml pepstatin; medium B/PIC). Embryos were solubilized in 1 ml of medium B/PIC containing 30 mM *n*-octylglucoside on ice for 2 h. To remove proteins that nonspecifically bound IgG, solubilized embryo proteins were incubated with 100 μg of preimmune IgG overnight at 4°C. The preimmune IgG–protein complexes were precipitated twice with protein A–Sepharose (100 μl of a 1:1 slurry) for 30 min at 4°C.

Solubilized embryo proteins pretreated with preimmune IgG were combined with an equal volume of 2 × polyacrylamide gel sample buffer containing bromophenol blue and 2 mM DTT, then heated to 37°C for 1 h. The samples were subjected to electrophoresis on 10% SDS–polyacrylamide gels, and separated proteins were transferred to nitrocellulose overnight at 30 V, 4°C. The nitrocellulose was incubated in 0.1 M Tris/0.9% NaCl buffer containing 0.2% Tween-20 (TTBS-T 20) and 5% normal goat serum for 2 h at room temperature followed by overnight incubation at 4°C with primary antibody (anti-avian GalTase IgG or preimmune IgG, 10 μg/ml) in TTBS-T 20 containing 5% normal goat serum. The nitrocellulose was rinsed for 1 h with TTBS-T 20 and incubated 2 h at 4°C in ^{125}I-goat anti-rabbit IgG (1×10^5 cpm/ml) in TTBS-T 20 containing 5% normal goat serum. The nitrocellulose was washed six times with TTBS-T 20, air dried, and exposed to x-ray film.

To determine whether chick embryo proteins identified by immunoblotting were in fact GalTase, enzyme activity was determined for proteins eluted from SDS gels. To increase the specific activity of the GalTase applied to the SDS gel, chick embryo GalTase was partially purified by α-lactalbumin affinity chromatography. 60 stage 18–20 chick embryos were solubilized in 4 ml of column buffer (0.1 M NaCl, 25 mM sodium cacodylate, 0.02% azide)/PIC, containing 1.0% Triton X-100, on ice for 4 h. Insoluble proteins were removed by centrifugation, and the supernatant was adjusted to a final concentration of 0.1% Triton X-100 by addition of column buffer/PIC. GalTase was purified by α-lactalbumin affinity chromatography as previously described (Hathaway et al., 1991), except that GalTase was eluted in column buffer without *N*-acetylglucosamine and containing 1.0 M NaCl. Peak fractions were pooled, lyophilized, resuspended in 3 ml dH_2O, and applied to a desalting column (model 10DG; Bio-Rad Laboratories, Richmond, CA). Fractions containing protein were pooled, lyophilized, resuspended in 100 μl SDS gel sample buffer containing 2 mM DTT, and then heated to 37°C for 1 h. 80% of the sample was applied to a single lane of a 10% SDS gel for elution and renaturation, and the remaining 20% was applied to two lanes for transfer to nitrocellulose and immunoblotting as described above. Following electrophoresis, the lane to be renatured was cut into 5-mm pieces; protein was eluted, precipitated, and renatured; and GalTase assays were conducted as described (Hathaway et al., 1991).

Immunoprecipitation and Inhibition of GalTase Activity by Anti-GalTase Antibodies

Stage 18–20 chick embryos were homogenized with a Polytron at a setting of 10 for 5 s, followed by 40 s at a setting of 6. Insoluble material was pelleted by centrifugation at 1,000 *g* for 5 min. Membranes were collected from the supernatant by centrifugation in an airfuge (Beckman Instr., Inc., Fullerton, CA) for 30 min at 200,000 *g*. For immunoprecipitation assays, 35 μg of total membrane protein was incubated with anti-GalTase IgG or preimmune IgG overnight at 4°C on a rotator in a total volume of 200 μl of medium B/PIC. Antigen/antibody complexes were precipitated with protein A–Sepharose (100 μl of a 1:1 slurry; Pierce, Rockford, IL). GalTase activity in the supernatant was assayed as previously described (Hathaway et al., 1991), using 100 μM unlabeled UDPgalactose, 1.0 μCi UDP[^{3}H]-galactose, 10 mM $MnCl_2$, and 30 mM *N*-acetylglucosamine. [^{3}H]Galactosylated reaction product was separated from unused UDP[^{3}H]galactose and its breakdown products by high-voltage borate electrophoresis, and radioactivity remaining at the origin was quantitated by liquid scintillation spectroscopy. Background radioactivity was determined by incubating a sample on ice in parallel, and this value was subtracted from all results.

For inhibition of enzyme activity, 100 μg of total membrane protein was incubated with anti-GalTase Fab or preimmune Fab for 1 h on ice with frequent agitation, in a total volume of 125 μl. GalTase assays were conducted on aliquots of the membrane-antibody mixtures as described above.

In vitro Migration Assays

Stage 8–10 chick embryos were collected as described above. Cranial neural tubes were isolated and were cultured in laminin-coated (10 μg/ml) 15-mm wells (Nunc Inc., Naperville, IL) for 24 h as previously described (Runyan et al., 1986). Neural crest cell migration assays were performed on an inverted microscope stage and were examined by time-lapse microphotography as previously described (Runyan et al., 1986). For each population of neural crest cells, a basal rate of migration was established. Culture medium was then replaced with medium containing the antibody reagent, and the migration rate was determined for the same population of cells. Anti-GalTase IgG and preimmune IgG were added at 500 μg/ml, and anti-GalTase Fab and preimmune Fab at 200 μg/ml. Data obtained from 35-mm time-lapse films was analyzed as previously described (Runyan et al., 1986).

Antibody Microinjection

Stage 6–9 embryos were prepared as described above for in vivo microinjection. To determine the distribution of microinjected IgG and Fab, embryos were injected with goat anti-rabbit IgG-FITC (1 mg/ml protein; Boehringer Mannheim Biochemicals, Indianapolis, IN) or goat anti-rabbit Fab-FITC (10 mg/ml protein; Organon Teknika, Rockville, MD) in PBS, into the embryonic head mesenchyme, lateral to the mesencephalon. Reagents were adjusted for optimal FITC concentration. 5 nl of antibody solution was backfilled into a glass needle with an internal diameter of 10–20 μm. Needles were made from 100-μl micropipets on a vertical micropipet puller (model 720; David Kopf Instrs., Tujunga, CA). The solution was injected with a pulse of air. Embryos were removed to a depression slide either immediately or after incubating for 1 h at 38°C. Embryos were viewed with epifluorescence on a microscope (model Dialux 22; E. Leitz, Inc., Rockleigh, NJ) equipped with a camera (model FX 35A; Nikon Inc., Melville, NY).

To determine the effects of blocking surface GalTase activity during embryonic development in vivo, antibodies were microinjected into the head mesenchyme of stage 7–9 chick embryos, lateral to the mesencephalon as described above. In some experiments, stage 6 embryos were microinjected just cranial to Henson's node. 5 nl of DME containing anti-GalTase IgG or Fab (1.3 mg/ml) or preimmune IgG or Fab (1.3 mg/ml) was injected into the right side of the embryo. Eggs were sealed and returned to the incubator as described above. Embryos were recovered after 4–24 h of incubation, fixed in Bouin's fixative for 24 h at room temperature, dehydrated through a graded series of ethanol, cleared in Hemo-DE (Fisher Scientific, Pittsburgh, PA), and embedded in Paraplast (Fisher Scientific). Embryos were serially sectioned through the transverse plane at 10 μm, mounted on gelatin-coated slides, and prepared for anti-HNK-1 immunofluorescence to visualize neural crest cells. Briefly, sections were deparaffinized with Hemo-DE and rehydrated through a graded series of ethanols to PBS. Slides were incubated for 15 min in PBS with 0.1% BSA. Sections were incubated in anti-HNK-1 (Abo and Balch, 1981) hybridoma culture supernatant overnight at 4°C, rinsed three times in PBS, incubated in goat anti-mouse IgM (1/50) for 1 h at room temperature, rinsed three times in PBS, and finally incubated in rabbit anti-goat IgG-FITC (1/50) for 1 h at room temperature. Slides were rinsed and mounted with glycerol/PBS (9:1) containing 4% *n*-propyl gallate and were then coverslipped. The sections were viewed with epifluorescence as described earlier. Following anti-HNK-1 immunofluorescence, the sections were stained with hematoxylin and eosin. Since cranial neural crest cells are not anti-HNK-1-immunoreactive in embryos younger than stage 10, these sections were stained with hematoxylin and eosin. In all cases, serial sections were examined from the cranial neuropore to the auditory vesicles.

Anti-GalTase Immunofluorescence

Stage 5–12 embryos were recovered as described above and fixed for 24 h at 4°C in St. Marie's fixative (Sainte-Marie, 1962). Embryos were dehydrated through 100% ethanol and embedded in Steedman's low-temperature embedding medium as described (Norenburg and Barrett, 1987). Sections were cut at 7 μm and floated onto gelatin-coated slides in dH_2O. The water was removed immediately, and the sections were dried at room temperature for 48 h. Embedding medium was removed with 100% ethanol, and the sections were rehydrated into PBS. Sections were incubated overnight at 4°C with anti-GalTase antisera or preimmune sera (1/50), diluted in PBS containing 5% normal goat serum. Slides were rinsed three times in PBS, then incubated in goat anti-rabbit IgG-FITC (1/50) for 1 h at room temperature. Slides were rinsed, coverslipped, and viewed as described above.

Alternatively, to visualize predominantly cell surface-associated GalTase, embryos were treated with antibodies before embedding using a technique modified from Martins-Green and Tokuyasu (1988). Embryos were cut transversely into several pieces with a scalpel, then fixed for 30 min at room temperature in Bouin's fixative. After rinsing 1 h in 70% ethanol and 1 h in 0.2 M phosphate buffer containing 0.02% NaN_3 and 0.002% Triton X-100 (the latter to serve as a surfactant) (PNT), aldehyde groups were blocked by incubation in PNT containing 0.1 M glycine for 30 min at room temperature. Embryos were incubated overnight at 4°C with anti-GalTase antisera or preimmune sera (1/50) in PNT containing 5% normal goat serum, washed for 6 h with PNT, incubated overnight at 4°C with goat anti-rabbit IgG-FITC (1/50) in PNT with 5% normal goat serum, and washed for 6 h in PNT. Finally, embryos were fixed again for 1 h, blocked with 0.1 M glycine, dehydrated through 100% ethanol, cleared in Hemo-DE, and embedded in Paraplast.

Results

Identification of Chick Embryo Membrane GalTase by Western Immunoblotting

The anti-GalTase antibody used in this study has been shown previously to react with avian GalTase from chicken serum and from chick embryo fibroblasts (Hathaway et al., 1991). The specificity of the antibody toward chick embryo GalTase was determined using solubilized whole stage 7–12 embryos (for Western immunoblotting) or membranes prepared from stage 7–12 embryos (for immunoprecipitation and inhibition assays). The anti-avian GalTase antibody recognized two proteins with apparent molecular masses of 77 and 67 kD on Western immunoblots (Fig. 1). Both the anti-GalTase and preimmune antibodies nonspecifically labeled several additional proteins, but these were eliminated by pretreating the solubilized embryos with preimmune IgG and protein A-Sepharose before gel electrophoresis (not shown). After preimmune IgG pretreatment, two nonspecifically labeled bands were still detected, at 55 kD (*asterisk*, Fig. 1) and at >85 kD (*double asterisk*, Fig. 1). The higher molecular weight band, which occurred as a result of preimmune IgG pretreatment, does not mask any proteins labeled specifically by anti-GalTase IgG, as assessed by immunoblots in which pretreatment with preimmune IgG was omitted (not shown).

To determine if these polypeptides are in fact GalTase, GalTase was identified in stage 18–20 embryos by elution and renaturation of α-lactalbumin-purified glycoproteins resolved by SDS-PAGE. GalTase activity was primarily associated with the 77- and 67-kD polypeptides that reacted specifically with the anti-GalTase IgG by Western blotting. Significant GalTase activity was not detectable in any other portion of the gel, including the two nonspecifically labeled bands. No protein bands were detectable on silver-stained gels between the 77- and 67-kD proteins, thus ruling out the possibility that another protein(s) not immunolabeled with anti-GalTase antibody was responsible for the GalTase activity (not shown). Similar results were obtained in three separate assays. The 77- and 67-kD proteins consistently showed high levels of activity, although they were not always equal to one another, supporting the notion that the two polypeptides are related by proteolysis, as is commonly found with mammalian GalTases (Smith and Brew, 1977). It is likely

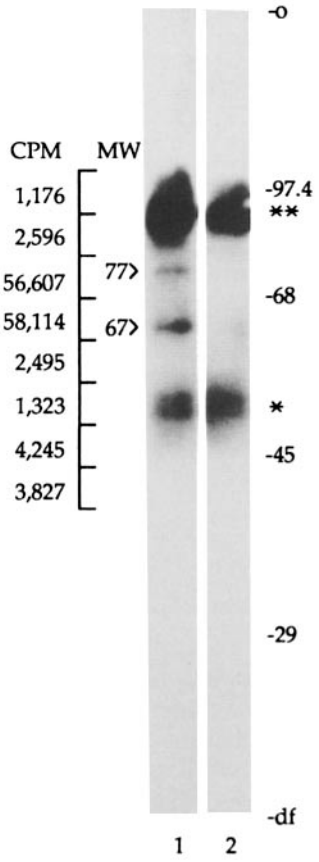

Figure 1. Identification of chick embryo GalTase by Western immunoblotting. Solubilized stage 7–12 chick embryos were pretreated with preimmune IgG and protein A–Sepharose, electrophoresed on 10% SDS polyacrylamide gels under reducing conditions, and transferred to nitrocellulose. Proteins were immunolabeled with polyclonal anti-avian GalTase IgG (lane *1*) or preimmune IgG (lane *2*), as described in Materials and Methods. Two proteins with apparent molecular masses of 77 and 67 kD were specifically labeled by the anti-GalTase antibody. As a result of preimmune IgG/protein A–Sepharose pretreatment, a nonspecific, high molecular weight protein was seen in both anti-GalTase-labeled and preimmune-labeled lanes (**). In addition, a band with apparent molecular mass of 55 kD nonspecifically labels with both anti-GalTase and preimmune IgG (*). Molecular mass was determined by linear regression analysis, and positions of molecular weight markers are indicated to the right: (*o*), origin; (*df*) dye front. To determine GalTase activity, protein was eluted from the gel and renatured, and GalTase assays were performed as described in Materials and Methods. Total cpm is indicated to the left of the gel, for each sample measured. Background radioactivity averaged 918 cpm and was subtracted from each sample.

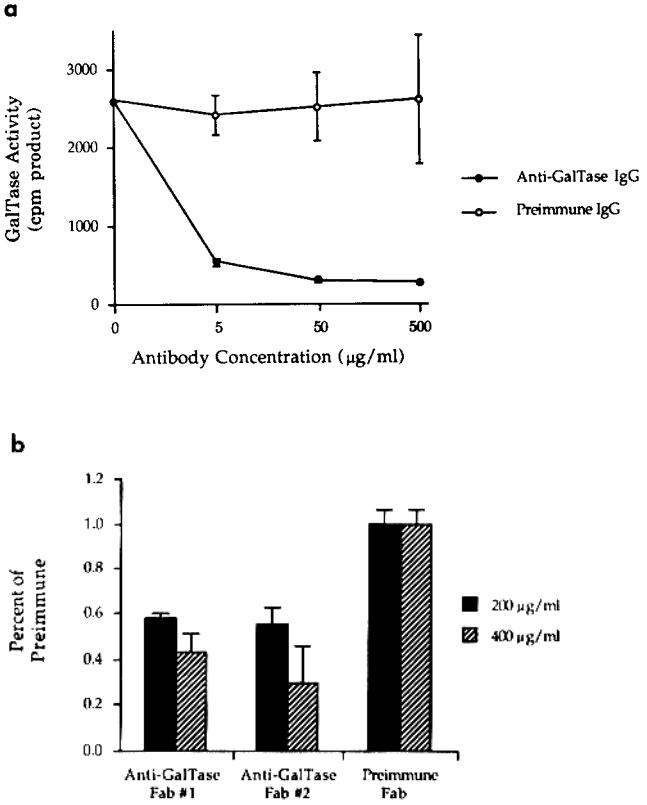

Figure 2. Immunoprecipitation and inhibition of chick embryo GalTase activity by anti-GalTase antibodies. (*A*) GalTase activity from stage 18–20 chick embryo membranes was precipitated with anti-GalTase IgG or preimmune IgG as described in Materials and Methods, and GalTase activity remaining in the supernatant was determined. 22% of the enzyme activity remained in the supernatant with 5 μg/ml anti-GalTase IgG, and 11% with 50 μg/ml IgG. No additional precipitation was observed with greater concentrations of antibody. Preimmune IgG had no effect on GalTase activity, compared to controls containing no antibody. background radioactivity averaged 119 cpm and was subtracted from each sample. (*B*) Membrane proteins prepared from stage 18–20 chick embryos were incubated in the presence of anti-GalTase Fab or preimmune Fab, and enzyme activity was determined as described in Materials and Methods. At 200 μg/ml Fab, GalTase activity was inhibited by 42 and 45%, compared to preimmune controls, and at 400 μg/ml, inhibition increased to 57 and 70%. The data are expressed as a percent of preimmune control. Actual cpm products for preimmune controls were 15,065 at 200 μg/ml and 18,339 at 400 μg/ml. Background radioactivity averaged 250 cpm and was subtracted from all samples.

that the 77-kD GalTase protein is the same protein as that affinity-purified from chick embryo liver (Furukawa and Roth, 1985), as judged by their migration relative to BSA standards.

Immunoprecipitation and Immunoinhibition of Chick Embryo GalTase Activity

The anti-avian GalTase antibodies have been shown previously to immunoprecipitate GalTase activity from chicken serum and from chick embryo fibroblasts (Hathaway et al., 1991). In this study, the anti-GalTase IgG was shown to immunoprecipitate chick embryo membrane GalTase activity as well, and in a dose-dependent manner (Fig. 2*A*). No enzyme activity was precipitated using preimmune IgG.

The anti-GalTase antibodies were also shown previously to inhibit GalTase activity toward both high molecular weight and monosaccharide substrates (Hathaway et al., 1991). As shown here, anti-GalTase Fab preparations also inhibited GalTase activity in chick embryo membranes and did so in a dose-dependent manner (Fig. 2*B*).

Neural Crest Cell Migration on Laminin Matrices In Vitro

Avian cranial neural crest cells have been shown to migrate on laminin in a GalTase-dependent manner (Runyan et al., 1986); therefore, this in vitro assay system was used to determine whether anti-GalTase antibodies can inhibit neural crest cell migration. Cranial neural crest cells were isolated and allowed to migrate onto laminin substrates in vitro as described in Materials and Methods. The rate of migration for a population of neural crest cells was determined in the presence and absence of anti-GalTase antibodies. Anti-GalTase Fab inhibited the rate of migration by 66%, from 54.4 to 23.7 μm/h (Fig. 3). Preimmune Fab had no significant effect on migration rate. Anti-GalTase IgG also inhibited migration (data not shown). Basal rates of migration in all assays were similar (52.1 ± 3.5 μm/h), and basal rates for the experimental and control population of cells within an assay

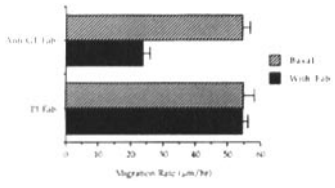

Figure 3. Anti-GalTase Fab inhibits neural crest cell migration on laminin in vitro. Neural crest cells were cultured on laminin matrices as described in Materials and Methods, and their migration rates were determined before and after addition of anti-GalTase Fab (*Anti-GT Fab*) or preimmune Fab (*PI Fab*). Migration rate in the presence of preimmune Fab did not change significantly (54.8 vs. 54.4 μm/h); however, migration rate decreased by 66%, from 54.4 to 23.7 μm/h, in the presence of anti-GalTase Fab. Bars indicate standard errors.

varied by <3.0 μm/h. The anti-GalTase and preimmune antibodies were shown to be nontoxic, since neural crest cells suffered no loss in viability after 24 h of culture in these reagents.

In summary, these results confirm earlier work that established a role for cell surface GalTase in avian neural crest cell migration on laminin matrices (Runyan et al., 1986). The experiments shown here also demonstrate that antibodies that inhibit chicken serum GalTase activity specifically recognize and inhibit chick embryo membrane GalTase activity, as well as inhibit surface GalTase activity in biological assays. The effects of anti-GalTase antibodies on chick embryo GalTase are both specific and dose-dependent, and are therefore appropriate reagents for testing the consequences of perturbing cell surface GalTase activity during development in vivo.

Distribution of IgG and Fab Microinjected into Chick Embryos

We initially determined the distribution of both IgG and Fab reagents injected into the chick embryo head mesenchyme. Fluoresceinated IgG or Fab was microinjected into the right side of stage 8–9 chick embryonic head mesenchyme, lateral to the mesencephalon. After 1 h, whole embryos were examined by fluorescence microscopy to visualize the antibody distribution. IgG was evenly distributed throughout the injected side of the head, but no label was detected on the uninjected side (Fig. 4 *a*), in agreement with studies by others demonstrating a unilateral distribution of microinjected IgG (Bronner-Fraser, 1985). The uninjected side therefore served as a positive control. In contrast, Fab injected into the right head mesenchyme became localized to both sides of the head after 1 h (Fig. 4 *b*), demonstrating that Fab fragments crossed the embryonic midline. Some embryos were examined immediately after microinjection to ensure that the bilateral distribution of the Fab was not due to microinjection error (not shown).

Anti-GalTase IgG Inhibits Neural Crest Cell Migration Unilaterally

Cranial neural crest cells initiate migration from the dorsal

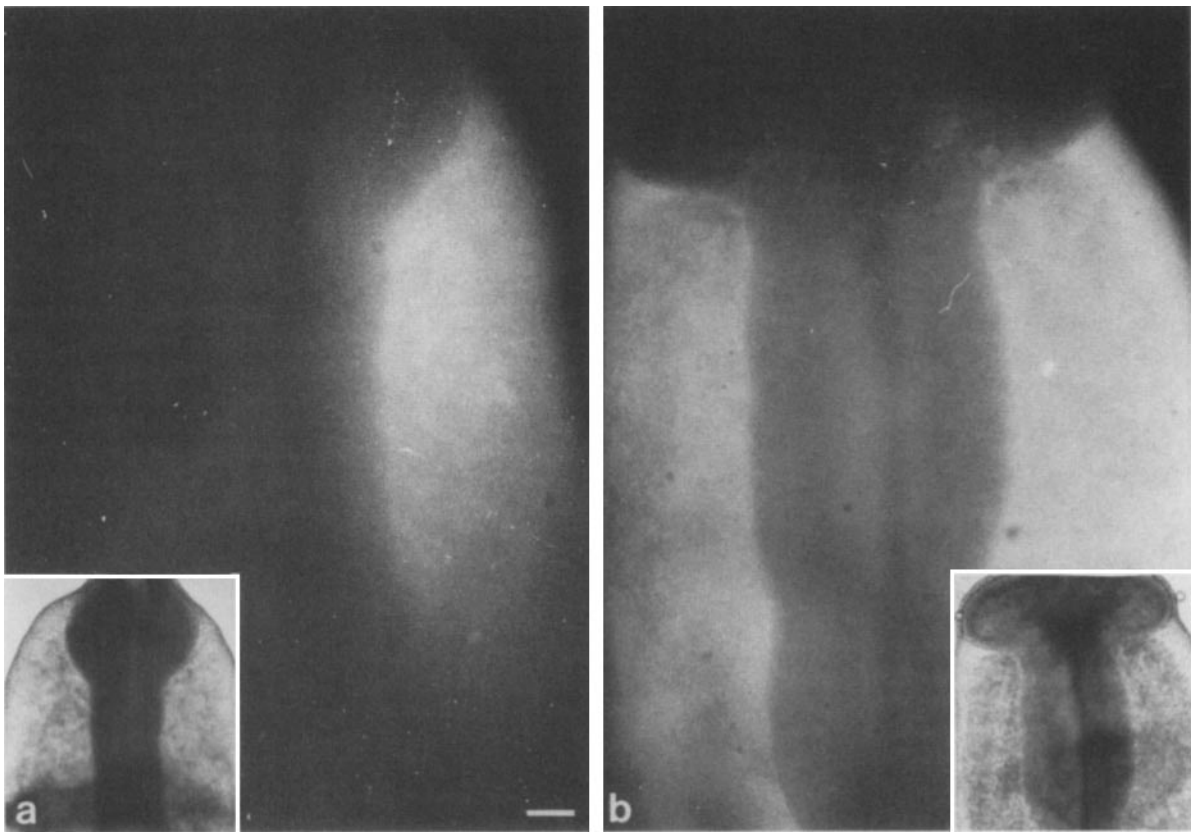

Figure 4. Distribution of IgG and Fab microinjected into chick embryos. Fluorescein-conjugated IgG or Fab was microinjected into stage 8–9 chick embryonic heads, in the right side of the mesenchyme lateral to the mesencephalon. After 1 h, the distribution of antibody was determined by fluorescence microscopy of whole embryos. IgG did not cross the midline to the left side (*a*), whereas Fab could be found throughout the head mesenchyme after 1 h (*b*). (*Insets*) Phase contrast views of the respective embryos. Bar, 50 μm.

Table I. Anti-GalTase Antibodies Inhibit Neural Development

Treatment	Number of Embryos	Number Normal	Number Abnormal*
Medium only	15	15(100%)	0
Preimmune IgG	16	15(94%)	1(6%)
Anti-GalTase IgG	15	5(33%)	10(67%)
Preimmune Fab	51	49(96%)	2(4%)
Anti-GalTase Fab	64	36(56%)	28(44%)‡

* For IgG-treated embryos, abnormal refers to neural crest cells on the injected side compared with the uninjected side.
‡ 39% of abnormal embryos had defective neural crest cell migration, 61% had neural tube defects, and 4% showed an overall inhibition of normal development.

aspect of the closing neural tube, moving laterally and ventrally beneath the skin ectoderm. Anti-GalTase IgG was microinjected into the pathway of migrating cranial neural crest cells on one side of the chick embryonic head mesenchyme. Control embryos were injected with preimmune IgG or medium alone. Embryos were incubated for an additional 4–8 h, harvested, and the neural crest cells visualized by anti-HNK-1 immunofluorescence on sections. The results from these experiments are presented in Table I. Whereas only 1 of 31 (3%) control-injected embryos showed any defect in neural crest cell migration, 10 of 15 (67%) embryos microinjected with anti-GalTase IgG showed abnormal cranial neural crest cell migration on the injected side of the embryo, compared with the uninjected side. Examples of IgG-injected embryos are shown in Fig. 5 and 6. In Fig. 5, *a* and *b*, an anti-GalTase IgG-injected embryo is shown at the level of the mesencephalon (midbrain) and the myelencephalon (hindbrain), respectively. The neural crest cells on the injected side (to the left in the micrograph) in this stage 11 embryo showed retarded ventrolateral migration. In addition, the neural crest cells have migrated in an anomalous position at the level of the hindbrain (Fig. 5 *b*), where they were in close contact with the neural tube on the injected side. A higher magnification view of a stage 10+ embryo comparing neural crest cell migration patterns on the anti-GalTase IgG-injected and uninjected sides of the same section is presented in Fig. 6. The neural crest cells on the injected side have not migrated as far ventrally as on the control side (Fig. 6, *arrows*). These observations are consistent throughout the midbrain and hindbrain regions of affected embryos, as assessed by examination of serial sections. No other developmental abnormalities were detected in embryos treated with anti-GalTase IgG.

Anti-GalTase Fab Inhibits Neural Crest Cell Migration Bilaterally

Anti-GalTase Fab was microinjected into the right head mesenchyme of stage 7–9 chick embryos. Stage 6 embryos were microinjected just cranial to Henson's node. Embryos were incubated for an additional 4–24 h, developing to

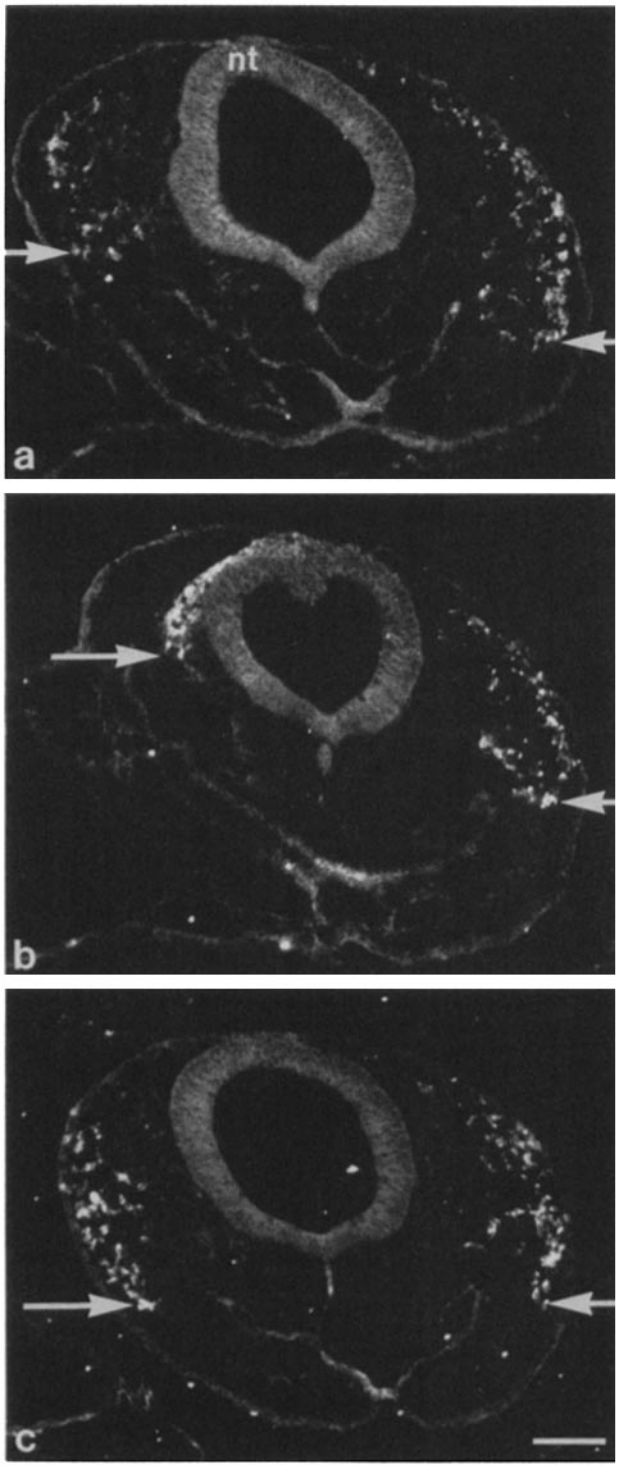

Figure 5. Anti-GalTase IgG inhibits neural crest cell migration unilaterally. Embryos were microinjected with IgG into the right head mesenchyme, lateral to the mesencephalon (the left side in the micrographs), and prepared for anti-HNK-1 immunofluorescence to visualize neural crest cells. (*a* and *b*) Cross-sections through the mesencephalon (*a*) and the myelencephalon (*b*) of the same stage 11 (13 somite) embryo treated with anti-GalTase IgG. The level of ventrolateral migration attained by the neural crest on the injected side was less than that on the uninjected side (*arrows*). Furthermore, neural crest cells migrated in an anomalous position in the hindbrain, where they were in close contact with the neural tube, compared with the neural crest on the uninjected side. (*c*) Embryos injected with preimmune IgG showed normal neural crest cell migration compared with the uninjected control side, as shown in a stage 11 embryo (*arrows*). Both embryos were incubated for 12 h following microinjection. nt, neural tube. Bar, 50 μm.

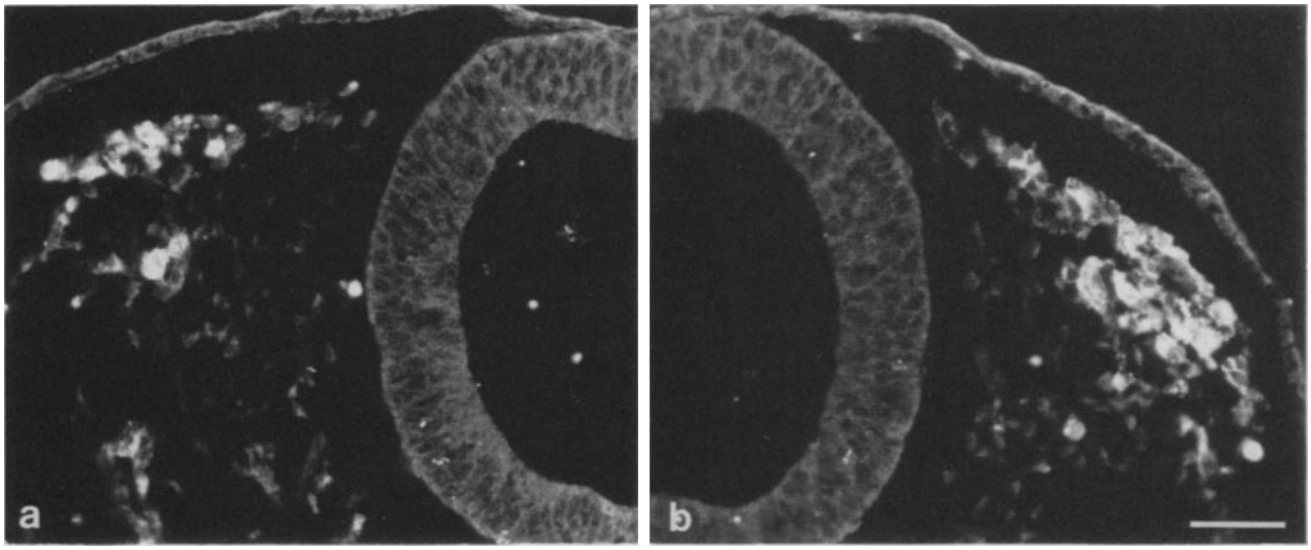

Figure 6. Anti-GalTase IgG inhibits neural crest cell migration unilaterally. Higher magnification view of a stage 10^+ (11 somite) embryo treated with anti-GalTase IgG, demonstrating unequal ventrolateral migration of the cranial neural crest cells on the injected side (*a*) compared with the uninjected side (*b*) of the same embryo. *a* and *b* are from the same section. Neural crest cells were visualized by anti-HNK-1 immunofluorescence. The position of neural crest cells shown in this panel is reflected throughout the mesencephalon and myelencephalon of this embryo, as judged by examination of serial sections. The embryo was incubated for 4 h following microinjection. Bar, 25 μm.

stages 8–15, harvested, and prepared for anti-HNK-1 immunofluorescence. The neural crest cells of embryos younger than stage 10 do not express anti-HNK-1 immunoreactivity; therefore, these embryos were stained with hematoxylin and eosin only.

Results from Fab microinjections of 115 embryos are presented in Table I. Only 2 of 51 (4%) preimmune-injected embryos demonstrated abnormalities in cranial neural crest cell migration. However, 28 of 64 (44%) embryos injected with anti-GalTase Fab demonstrated defects in neural crest cell migration or neural tube formation. 39% of affected embryos showed defects in neural crest cell migration. A wider range of embryonic ages was examined in Fab microinjection assays, and consequently, fewer of these embryos had neural crest defects compared with embryos injected with IgG. Some Fab-injected embryos were harvested before significant neural crest cell migration had begun, and many were allowed to develop 20–24 h after injection, perhaps allowing

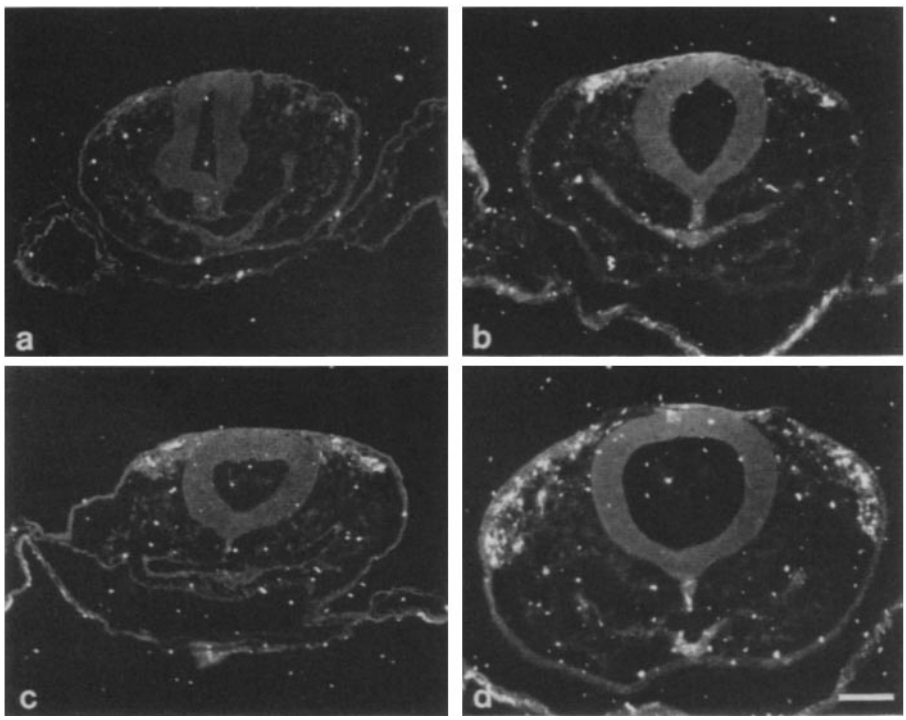

Figure 7. Anti-GalTase Fab inhibits neural crest cell migration bilaterally. Embryos microinjected with anti-GalTase Fab to the right side of the mesenchyme lateral to the mesencephalon demonstrate bilaterally decreased neural crest cell migration (*a* and *c*), compared with age-matched embryos microinjected with preimmune Fab (*b* and *d*). *a* and *b* are stage 10^- (9 somites) and *c* and *d* are stage 10^+ (11 somite) embryos. Neural crest cells were visualized by anti-HNK-1 immunofluorescence. All embryos were incubated for 7 h after microinjection. Bar, 50 μm.

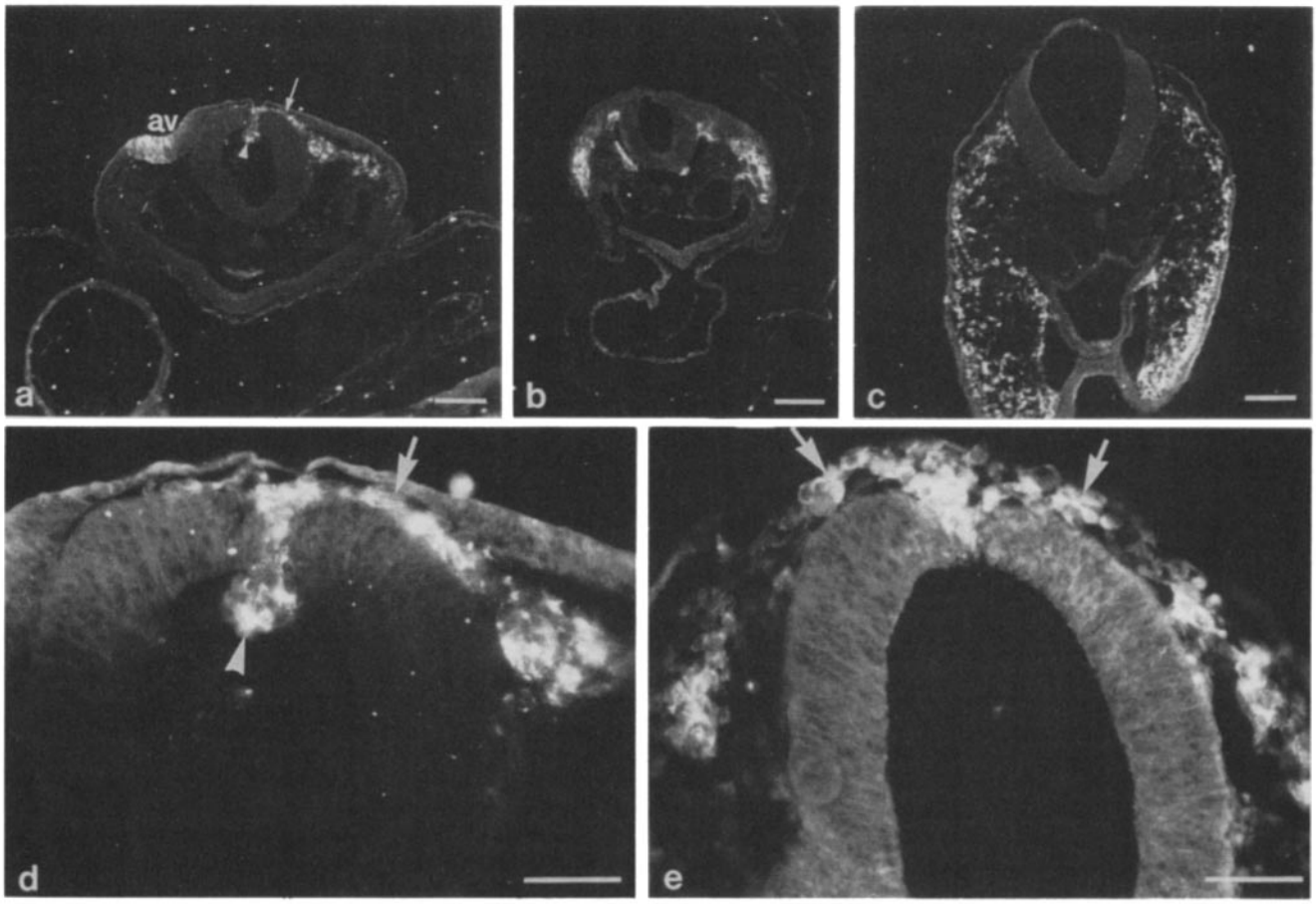

Figure 8. Neural crest cell migration defects associated with anti-GalTase Fab. (*a* and *d*) The same stage 12 anti-GalTase Fab-treated embryo at different magnifications. Neural crest cells remained associated with the dorsal neural tube (*arrows*) and entered the neural tube (*arrowheads*). (*b*) A preimmune Fab-treated embryo at the same stage. These embryos were incubated for 20 h following microinjection. The section shown in *a* was cut at an oblique angle showing the auditory vesicle (*av*). (*e*) The embryo was incubated for 12 h following microinjection, developing to stage 13^- (18 somites). Neural crest cells remained associated with the dorsal neural tube (*arrows*). (*c*) An age-matched preimmune Fab-treated embryo. Neural crest cells all migrated ventrolaterally away from the neural tube. Neural crest cells were visualized by anti-HNK-1 immunofluorescence. Bars: 50 μm (*a–c*); 25 μm (*d* and *e*).

sufficient dilution of the Fab and recovery of neural crest cell migration. Except for the observed perturbation of neural crest cell migration and neural tube defects discussed below, longer term development (i.e., 20–24 h after injection) of anti-GalTase Fab-treated embryos appeared normal and comparable to age-matched controls in all but two embryos (4%).

Fig. 7 depicts stage 10^- (Fig. 7, *a* and *b*) or stage 10^+ (Fig. 7, *c* and *d*) embryos microinjected with anti-GalTase Fab (Fig. 7, *a* and *c*) or preimmune Fab (Fig. 7, *b* and *d*) and incubated for 7 h following injection. The cranial neural crest cells of the anti-GalTase-treated embryos did not migrate as far ventrolaterally as the neural crest cells in the control embryos. The reduced size of the anti-GalTase Fab-treated heads may be due to the reduced migration of the neural crest.

Neural crest cells in anti-GalTase Fab-treated embryos were frequently found associated with the dorsal neural tube, long after these cells have migrated away from this area in normal embryos (Fig. 8). The cranial neural crest cells in anti-GalTase Fab-injected embryos (Fig. 8, *a*, *d*, and *e*) did not completely migrate away from the dorsal neural tube, and some cells entered the neural tube. Neural crest cell distribution was normal in preimmune Fab-injected embryos (Fig. 8, *b* and *c*).

Collectively, these results suggest that perturbation of cell surface GalTase activity inhibits the initial stages of neural crest cell migration. Once migration has commenced, i.e., at stage 10 or later, cranial neural crest cells were not affected by perturbation of cell surface GalTase (not shown). These results support a function for cell surface GalTase during initial emigration of cranial neural crest cells away from the dorsal neural tube.

Anti-GalTase Fab Disrupts Neural Tube Formation

In addition to inhibiting migration of cranial neural crest cells, injection of anti-GalTase Fab into the head mesenchyme resulted in neural tube defects in 61% of treated embryos. Neural tubes developed normally in 100% of control embryos. The defects are best summarized as an abnormal neural fold elevation and lateral hinge plate formation (Schoenwolf and Smith, 1990), and incomplete neural tube closure. Anti-GalTase Fab-injected, hematoxylin and eosin-stained embryos are shown in Fig. 9, *a*, *b*, and *d*, at stage

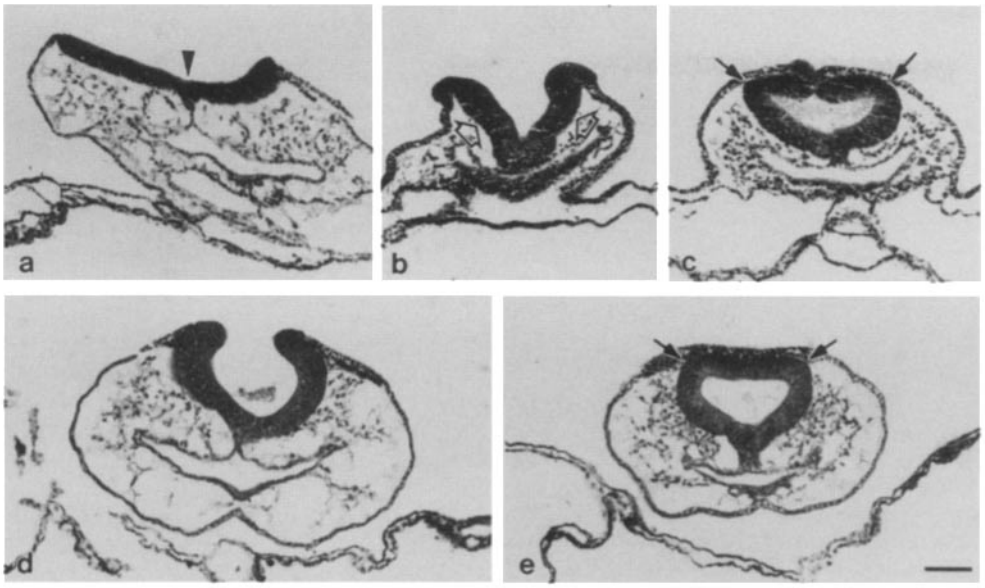

Figure 9. Anti-GalTase Fab disrupts normal neural tube formation. (*a–c*) Embryos were microinjected with Fab at stage 6, just cranial to Henson's node, and harvested after 4 h, at stage 8^+ (five somites). Anti-GalTase Fab caused incomplete neural tube closure (*a* and *b*), whereas preimmune Fab-treated embryos were normal (*c*). In *a*, median hinge formation has occurred normally (*arrowhead*), but neural folds have not elevated. In *b*, neural fold elevation has proceeded normally (*open arrowheads*), but lateral hinge formation has failed. Normal lateral hinge formation is seen in control embryos (*c*, *arrows*). (*d* and *e*) The embryos were microinjected at stage 8 and incubated for an additional 6 h to stage 10^- (9 somites). Lateral hinge formation was abnormal in the anti-GalTase Fab-treated embryo (*d*), as compared with embryos treated with preimmune Fab (*e*, *arrows*). Development otherwise appeared normal. Sections were stained with hematoxylin and eosin. Bar, 50 μm.

8^+ (Fig. 9, *a* and *b*) or stage 10^- (Fig. 9 *d*). Age-matched preimmune Fab-injected controls are also shown (Fig. 9, *c* and *e*). Neural tube closure was incomplete in anti-GalTase Fab-treated embryos due to a failure of neural fold elevation (Fig. 9 *a*) or lateral hinge formation (Fig. 9, *b* and *d*). A stage 13^+ embryo, incubated for 20 h after microinjection with anti-GalTase Fab (Fig. 10, *a*, *c*, and *d*), had an open neural tube in the forebrain region, and HNK-1–positive neural crest cell material had entered the hindbrain (Fig. 10 *c*). Development otherwise appeared normal in this embryo, indicating that anti-GalTase perturbation of neural tube closure persists in the absence of any obvious secondary defects. Finally, some anti-GalTase Fab–injected embryos showed bifurcated neural tubes resulting from inward folding of the dorsal neural tube (Fig. 11).

In summary, treatment of embryos with anti-GalTase antibodies affects neural crest cell migration unilaterally (IgG) or bilaterally (Fab) compared to embryos microinjected with preimmune antibodies. These effects correlate well with the distribution of microinjected IgG and Fab reagents. Serial sections were examined for all embryos, and affected embryos showed neural crest cell defects in large regions of the mid- and hindbrain areas. Most of the defects consisted of reduced or anomalous migration of neural crest cells, although some embryos appeared to have a reduced volume of neural crest cells. The volume of HNK-1 positively stained cells was determined for two representative IgG-injected embryos, and was found to be reduced by 29 and 14% on the injected side. Because of these small differences, and because quantitation of HNK-1–immunoreactive regions is imprecise owing to the loose association of neural crest cells, determination of neural crest cell volume was not continued. Finally, anti-GalTase Fab affected neural tube development, resulting in abnormal neural fold elevation and incomplete or improper neural tube closure.

Indirect Immunofluorescence Localization of GalTase

The distribution of GalTase was determined by indirect immunofluorescence on serially sectioned embryos that had been embedded in low-temperature embedding medium. GalTase was localized to most cell types, as expected, since GalTase is a component of the Golgi apparatus (Fig. 12). Before the onset of migration, presumptive cranial neural crest cells did not express significant levels of anti-GalTase immunoreactivity (Fig. 12 *a*); however, label was associated with these cells as they began to migrate away from the dorsal neural tube (Fig. 12 *c*). GalTase immunoreactivity was heaviest on the leading cells of the migratory neural crest cell cluster (Fig. 12 *c*), and they continued to express GalTase at later stages of migration (Fig. 12 *d*). The migratory head mesenchyme also expressed GalTase (Fig. 12, *a*, *c*, and *d*). Comparison to anti-HNK-1 labeling, an epitope localized exclusively to the cell surface (Vincent and Thiery, 1984), in double-label experiments suggests that a high proportion of the GalTase on these migratory cell types is associated with the cell surface (not shown). In addition, GalTase was localized to the interface between the neural epithelia and the ectoderm (Fig. 12 *g*), to the basal surfaces and regions of neural epithelial cells (Fig. 12 *h*), as well as to the basal surface of the notochord, gut endoderm, and vascular endothelium in older embryos (Fig. 12 *h*). Finally, anti-GalTase immunofluorescence was detectable on the apical surfaces and regions of ectodermal cells (Fig. 12, *c*, *d*, and *g*), which may represent a secretory form of GalTase often associated with secretory epithelia (Roth et al., 1985).

A preembedding immunofluorescence technique was used to enhance the visualization of GalTase associated with basal lamina (Martins-Green and Tokuyasu, 1988). Anti-GalTase antibody heavily labeled the basal surfaces of neural epithelial cells of early neurula-stage embryos (stages 7–8; Fig. 12

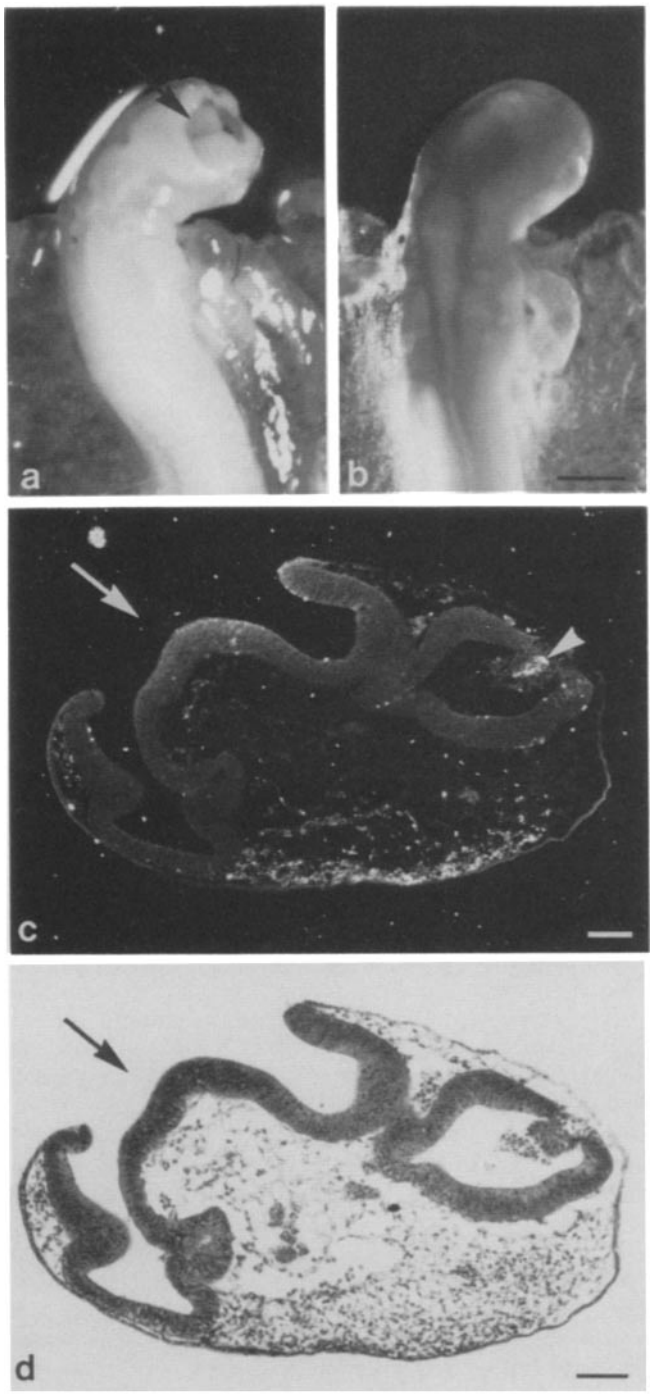

Figure 10. Anti-GalTase Fab disrupts neural tube formation. The stage 13^+ (20 somite) embryo whole mount shown in *a* was microinjected with anti-GalTase Fab at stage 8 and incubated for an additional 20 h. The neural tube in the forebrain region (*arrow*) remained open. A control stage 13^- (18 somite) embryo microinjected with preimmune Fab, shown in *b*, appeared normal. The embryo in *a* was serially sectioned and prepared for anti-HNK-1 immunofluorescence (*c*) and for hematoxylin and eosin staining (*d*). The open neural tube of the forebrain is evident (*arrows*), and some HNK-1–positive neural crest cell material has entered the neural tube in the hindbrain region (*c*, *arrowhead*). Neural crest cell migration and development otherwise appeared normal in this embryo. Bars: 500 μm (*a* and *b*); 50 μm (*c* and *d*).

e). Control sections treated with preimmune sera demonstrated no detectable fluorescence associated with the basal neural epithelia (Fig. 12, *b* and *f*).

Discussion

Our interest in cell surface GalTase function during embryonic development is based upon previous work demonstrating that GalTase is present at high levels on the surface of migrating cells and between cells and tissues undergoing inductive interactions (Shur, 1977). These results suggested that cell surface GalTase might participate during these events. Subsequent in vitro studies showed that GalTase participates during neural crest cell migration on laminin matrices (Runyan et al., 1986). However, it is necessary to determine whether molecular models for cell–matrix interactions developed in vitro are actually functional during development in vivo. Consequently, in this study we examined the role of cell surface GalTase during neural crest cell migration and neural development in vivo. The antibody used in these experiments was raised in rabbits against chicken serum GalTase purified to apparent homogeneity (Hathaway et al., 1991). The polyclonal antibody recognized avian GalTase as determined by several criteria, including ELISA, immunoprecipitation of enzyme activity from serum and chick embryo fibroblasts, inhibition of enzyme activity, and by Western immunoblotting (Hathaway et al., 1991). In this study, the antibody specifically recognized chick embryo GalTase as shown by Western blotting polypeptides that contained GalTase enzymatic activity following renaturation. The antibodies also inhibited chick embryo membrane GalTase activity in a dose-dependent manner, suggesting that the polyclonal antibodies recognize epitopes at or near the active site.

The efficacy of these antibodies for in vivo studies was established using an appropriate in vitro assay. Cranial neural crest cells migrate on laminin in a GalTase-dependent manner, since migration is inhibited by the GalTase modifier protein α-lactalbumin and by competitive substrates, and is enhanced by the sugar nucleotide substrate, UDPgalactose (Runyan et al., 1986). Anti-GalTase IgG and Fab both significantly inhibited the migration of these cells in vitro, without affecting viability. These antibodies are therefore specific, inhibitory, nontoxic, and react with GalTase in a dose-dependent, saturable manner.

The distribution of IgG and Fab reagents was established by microinjection into the head mesenchyme of stage 8–9 chick embryos. IgG did not cross the embryonic midline after 1 h of incubation, in agreement with published findings (Bronner-Fraser, 1985). On the other hand, Fab crossed the midline within 1 h of incubation. The inability of IgG to cross the midline may simply reflect its larger size relative to Fab fragments, which quickly diffuse throughout the head. Alternatively, putative Fc-binding sites on embryonic cells may prevent IgG from diffusing far from the site of injection.

Anti-GalTase IgG was microinjected into the chick embryonic head mesenchyme, lateral to the mesencephalon of stage 7–9 embryos. Neural crest cell migration was affected only on the injected side of the embryo. Neural crest cell migration was also perturbed with anti-GalTase Fab, but both sides of the embryo were affected. In some cases, neural

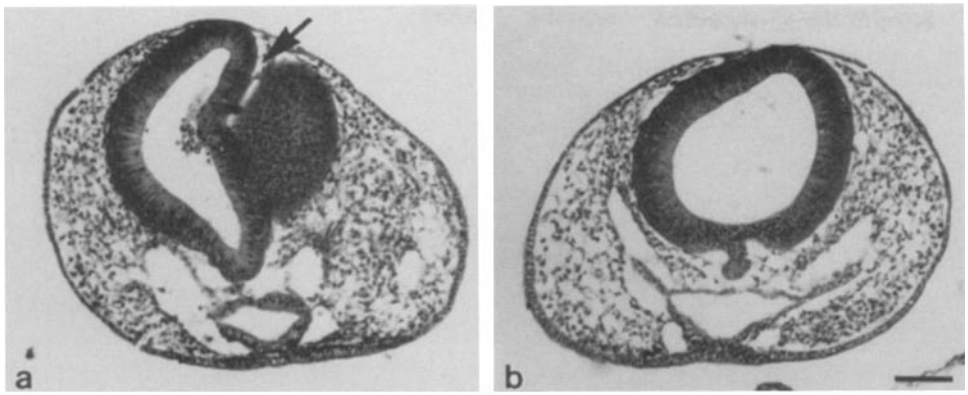

Figure 11. Anti-GalTase Fab induces abnormal neural tube closure. (*a*) In some anti-GalTase Fab–treated embryos, neural tube closure resulted in a dorsally bifurcated neural tube, possibly resulting from an overrotation of the dorsal neural folds (*arrow*), as shown in this stage 11^+ (14 somite) embryo incubated for 20 h following antibody treatment. (*b*) An age-matched control-treated embryo, with normal neural tube closure. Sections were stained with hematoxylin and eosin. Bar, 50 μm.

crest cells were observed in anomalous positions, such as within the neural tube, dorsal to the neural tube after ventrolateral migration would normally have been completed, or in contact with the lateral neural tube rather than in contact with the ectoderm.

GalTase immunoreactivity was low on neural crest cells before the onset of migration, but appeared on the leading cells in the neural crest population as they initiated migration away from the dorsal neural tube. A comparison of the pattern of anti-GalTase and anti–HNK-1 immunoreactivities on the same sections suggests that a significant portion of the GalTase resides on the cell surface. This conclusion is supported by the fact that migratory neural crest cells express cell surface GalTase activity (Runyan et al., 1986), although the relative amount of cell surface and intracellular GalTase in neural crest cells has not been determined. Collectively, these data suggest that cell surface GalTase may function during the initial migration of neural crest cells away from the neural tube. During this time, neural crest cells are in closest contact with a laminin-rich basal lamina that lines the basolateral surface of both the ectoderm and the neural tube (Duband and Thiery, 1987; Martins-Green and Erickson, 1987). Since GalTase mediates cell–laminin interactions in vitro, our data are consistent with the hypothesis that surface GalTase on migratory cranial neural crest cells mediates, in part, their interaction with laminin within the basal lamina of adjacent epithelia and within the extracellular matrix, thus influencing migration. This is further supported by the fact that the E8 domain of laminin supports neural crest cell migration (Perris et al., 1989), and has been identified as the surface GalTase-binding site within laminin (Begovac et al., 1991). In vitro studies have shown that laminin induces surface GalTase expression on migrating mesenchymal cells (Eckstein and Shur, 1989), raising the possibility that the basal lamina may induce surface GalTase expression on adjacent neural crest cells, thus initiating migration.

An in vivo study is usually not well suited to quantitation, however the overall extent and type of neural crest cell defect seen in this study appears to reflect a decrease in the rate of migration of this cell type. The most commonly seen defect was reduced ventrolateral migration of neural crest cells on the injected side of the embryo (IgG studies) or compared to age-matched preimmune controls (Fab studies). This reduction was never absolute; some migration of neural crest cells was always observed in affected embryos. Although we cannot rule out the possibility that the anti-GalTase reagent becomes diluted so as to allow some recovery of migration by the earliest observation time (4 h), these results suggest that cell surface GalTase is one of several cell surface receptors involved in mediating neural crest cell migration in vivo. In light of the work of others (Boucat et al., 1984; Bilozur and Hay, 1988; Bronner-Fraser, 1985, 1987; Bronner-Fraser and Lallier, 1988) demonstrating roles for other cell surface receptors and extracellular matrix components in neural crest cell migration, a cooperative, partially overlapping series of cell–matrix events is most probable.

This notion is further supported by the fact that the migratory defects produced by anti-GalTase antibodies showed subtle, but characteristic, differences from those produced by antibodies against other cell surface receptors and matrix components. Antibodies against integrin (Bronner-Fraser, 1986), the HNK-1 epitope (Bronner-Fraser, 1987), or the laminin-heparin sulfate proteoglycan complex (Bronner-Fraser and Lallier, 1988) all produced ectopic neural crest cells; a defect rarely seen after anti-GalTase antibody treatment. Since surface GalTase participates exclusively during cell spreading and migration, and not during initial cell attachment to laminin which involves other matrix receptors (Runyan et al., 1988), it is possible that defects following anti-GalTase treatment directly reflect defects in migration, and not secondary defects in cell–cell or cell–matrix adhesions.

A few embryos treated with anti-GalTase antibodies had a small reduction in neural crest cell volume associated with decreased migration. Others have reported similar findings using antibodies against different cell surface receptors to inhibit cranial neural crest cell migration (Bronner-Fraser, 1986, 1987). Reduced neural crest cell volume is not a primary defect of anti-GalTase antibody treatment, since not all embryos showing defective migration showed concomitant decreases in neural crest volume. It is not clear in either the present study or in others, if the reduced neural crest cell volume is due to fewer cells or due to neural crest cells clustering together as a result of antibody perturbation. Any effects on neural crest volume or cell number were not due to anti-GalTase antibody toxicity, since these reagents had no effect on the viability of cultured neural crest cells (the present study) or cultured chick embryo fibroblasts (unpublished observations), nor did these reagents affect neural crest volume, cell number or migration after stage 10 of development, although these cells are still dividing (Maxwell, 1976).

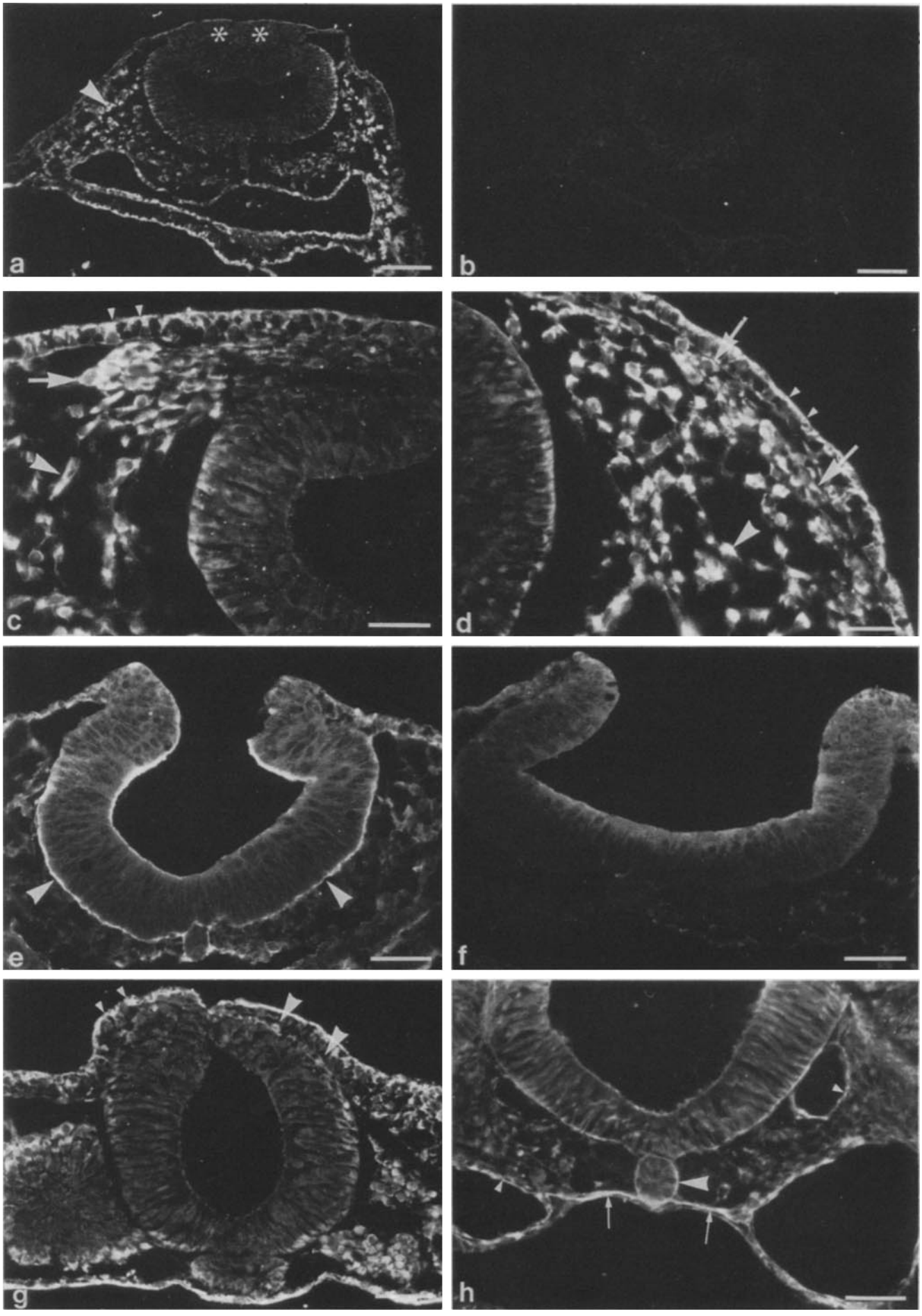
a
b
c
d
e
f
g
h

The inability of anti-GalTase antibodies to affect neural crest migration during later stages of development (after stage 10) is similar to that reported by others using antibodies against the HNK-1 epitope (Bronner-Fraser, 1987) and a laminin-heparin sulfate proteoglycan complex (Bronner-Fraser and Lallier, 1988). Cranial neural crest is actively migrating at stage 10, and GalTase immunoreactivity is detectable on these cells. Furthermore, GalTase is found on actively migrating head mesenchymal cells, however mesenchymal cell migration is not affected by blocking surface GalTase activity. Collectively, these results further suggest a functional redundancy, or overlap, of cell surface receptors during later stages of cranial neural crest cell migration and during mesenchymal cell migration. A similar phenomenon has been proposed in *Drosophila* nervous system development. Fasciclin I, a membrane-associated glycoprotein expressed on many neural cell types, mediates cell–cell adhesion in transfected cells, yet the complete loss of the gene product in vivo results in a normal nervous system phenotype, suggesting that other adhesion molecules participate in the same developmental processes (Elkins et al., 1990). It is equally likely that neural crest cell migration in stage 10 or older embryos may rely on as yet undefined cell-matrix or cell-cell receptors.

In addition to perturbing neural crest cell migration, anti-GalTase Fab treatment had a significant effect on neural tube formation. In 61% of the embryos examined, neural tubes either failed to close or closed abnormally, resulting in a dorsally bifurcated neural tube. Martins-Green (1988) and Schoenwolf and Smith (1990) have described three critical and independent events during cranial neural tube formation in chick embryos: (*1*) median hinge formation resulting from interactions between the neural plate and notochord, (*2*) elevation of the neural folds, and (*3*) lateral hinge formation resulting in the apposition of the dorsal neural folds (Smith and Schoenwolf, 1989; Placzek et al., 1990). The simplest explanation for the effects of anti-GalTase Fab on neural tube development is that cell surface GalTase is required for neural fold elevation, lateral hinge formation, or both, since median hinges formed normally in this study. (It is possible that anti-GalTase Fab was injected after the sensitive period). Neural fold elevation was inhibited in the youngest embryos treated with anti-GalTase Fab, whereas lateral hinge formation was affected in the majority of Fab-injected embryos showing neural tube defects. The dorsolateral hinges form at the point where ectoderm and neural folds are in contact (Martins-Green, 1988; Schoenwolf and Smith, 1990), an area rich in several extracellular matrix molecules (Tucker et al., 1988), particularly laminin (Martins-Green and Erickson, 1987), and GalTase immunoreactivity. Therefore, it is possible that cell surface GalTase may participate in neural tube formation by interacting with laminin in the basal lamina.

Neural tube defects were seen only with Fab treatment but not with IgG treatment, an observation for which there are several possible explantations. Anti-GalTase Fab was a more potent inhibitor of neural crest cell migration on laminin in pilot in vitro studies; therefore, it may have been a more potent inhibitor of cell surface GalTase function in vivo. Alternatively, there is evidence to suggest that neural tube formation can occur normally if one side of the neural tube is mechanically separated at the presumptive neural epithelial/ectodermal interface; neurulation is completely inhibited only if both sides are perturbed (Schoenwolf and Smith, 1990). Because IgG did not cross the midline, this reagent may have been prevented from producing neural tube defects.

In summary, cell surface GalTase appears to participate in cranial neural crest cell migration, perhaps by interacting with laminin in the embryonic basal lamina, in the extracellular space, or both. In addition, cell surface GalTase plays an as yet undefined role in early neural tube formation. It is unlikely that defects in neural crest cell migration are a secondary result of defective neurulation, since neural crest cell defects were often found in embryos with normal neurulation, particularly with IgG-treated embryos. One possibility is that surface GalTase on neural epithelia interacts with laminin within the basal lamina of the neural tube and that this interaction is critical for proper neural tube closure. Studies are currently under way to determine the distribution of GalTase at the ultrastructural level, and to address in detail the role of cell surface GalTase during neural development using in vitro whole embryo culture systems.

We would like to thank Courtney Cook for assistance in microinjections to determine antibody distribution, and Dr. Marianne Bronner-Fraser for HNK-1 hybridoma cells.

This work was supported by grant DE 07120 from the National Institutes of Health to B.D. Shur and by Institutional NRSA HDO7325 to H. J. Hathaway.

Received for publication 23 May 1991 and in revised form 23 January 1992.

Figure 12. Immunofluorescence localization of GalTase on sectioned embryos. (*a*) Before the onset of migration, neural crest cells associated with the dorsal neural tube (*) did not label for GalTase. (*c*) However, GalTase was expressed as migration began, particularly at the leading edge of the cluster of migrating neural crest cells (*arrow*). (*d*) At later stages of neural crest cell migration, neural crest cells retained high levels of GalTase expression (*arrows*). (*e*) Anti-GalTase immunoreactivity on the basal surfaces of neural epithelial cells was best seen in younger (stage 8^-) embryos with a preembedding immunofluorescence technique described in Materials and Methods. The basal surface of neural epithelial cells was heavily labeled for GalTase (*arrowheads*) during neural tube closure. (*g*) GalTase reactivity was also localized to the interface between the neural epithelial basal surface and the overlying ectoderm as the neural folds become apposed (*large arrowheads*). (*h*) GalTase was localized to basal surfaces of several cell types in older (stage 11^+) embryos, including the basal neural epithelium, the notochord (*arrowhead*), the gut endoderm (*small arrows*), and the vascular endothelium (*small arrowheads*). Actively migrating head mesenchymal cells (*a*, *c*, and *d*, *large arrowheads*) also labeled for GalTase, as did the apical surfaces and regions of ectodermal cells (*c*, *d*, and *g*, *small arrowheads*), which are presumably secreting Golgi-derived GalTase. (*b* and *f*) Control sections were incubated with preimmune sera and demonstrate nonspecific background levels of immunoreactivity. *a–d*, *g*, and *h* were embedded in low-temperature medium and reacted with antibodies after sectioning, and *e* and *f* were reacted with antibodies prior to embedding, all as described in Materials and Methods. Bars: 50 μm (*a* and *b*); 25 μm (*c–h*).

References

Abo, T., and C. M. Balch. 1981. A differentiation antigen of human NK and K cells identified by a monoclonal antibody (HNK-1). *J. Immunol.* 127: 1024–1029.

Austin, J., and J. Kimble. 1987. glp-1 is required in the germ line for regulation of the decision between mitosis and meiosis in *C. elegans*. *Cell.* 51:589–599.

Bayna, E. M., J. H. Shaper, and B. D. Shur. 1988. Temporally specific involvement of cell surface β1,4 galactosyltransferase during mouse embryo morula compaction. *Cell.* 53:145–157.

Begovac, P. C., and B. D. Shur. 1990. Cell surface galactosyltransferase mediates the initiation of neurite outgrowth from PC12 cells on laminin. *J. Cell Biol.* 110:461–470.

Begovac, P. C., D. E. Hall, and B. D. Shur. 1991. Laminin fragment E8 mediates PC12 cell neurite outgrowth by binding to cell surface β1,4 galactosyltransferase. *J. Cell Biol.* 113:637–644.

Bilozur, M. E., and E. D. Hay. 1988. Neural crest migration in 3D extracellular matrix utilizes laminin, fibronectin, or collagen. *Dev. Biol.* 125:19–33.

Boucat, J.-C., T. Darribere, T. J. Poole, H. Aoyama, K. M. Yamada, and J. P. Thiery. 1984. Biologically active synthetic peptides as probes of embryonic development: a competitive peptide inhibitor of fibronectin function inhibits gastrulation in amphibian embryos and neural crest cell migration in avian embryos. *J. Cell Biol.* 99:1822–1830.

Bronner-Fraser, M. 1985. Alterations in neural crest migration by a monoclonal antibody that affects cell adhesion. *J. Cell Biol.* 101:610–617.

Bronner-Fraser, M. 1986. An antibody to a receptor for fibronectin and laminin perturbs cranial neural crest development *in vivo*. *Dev. Biol.* 117:528–536.

Bronner-Fraser, M. 1987. Perturbation of cranial neural crest migration by the HNK-1 antibody. *Dev. Biol.* 123:321–331.

Bronner-Fraser, M., and T. Lallier. 1988. A monoclonal antibody against a laminin-heparan sulfate proteoglycan complex perturbs cranial neural crest migration in vivo. *J. Cell Biol.* 106:1321–1329.

Drake, C. J., and C. D. Little. 1991. Integrins play an essential role in somite adhesion to the embryonic axis. *Dev. Biol.* 143:418–421.

Duband, J.-L., and J. P. Thiery. 1987. Distribution of laminin and collagens during avian neural crest development. *Development (Camb.).* 101:461–478.

Dutt, A., J.-P. Tang, and D. D. Carson. 1987. Lactosaminoglycans are involved in uterine epithelial cell adhesion *in vitro*. *Dev. Biol.* 119:27–37.

Eckstein, D. J., and B. D. Shur. 1989. Laminin induces the expression of surface galactosyltransferase on lamellipodia of migrating cells. *J. Cell Biol.* 108:2507–2517.

Eckstein, D. J., and B. D. Shur. 1992. Cell surface β1, 4 galactosyl-transferase is associated with the detergent-insoluble cytoskeleton on migrating mesenchymal cells. *Exp. Cell Res.* In press.

Elkins, T., K. Zinn, L. McAllister, F. M. Hoffmann, and C. S. Goodman. 1990. Genetic analysis of a Drosophila neural cell adhesion molecule: interaction of fasciclin I and Abelson tyrosine kinase mutations. *Cell.* 60:565–575.

Flanagan, J. G., D. Chan, and P. Leder. 1991. Transmembrane form of the *kit* ligand growth factor can be regulated by alternative splicing and is deleted in the Sl^d mutant. *Cell.* 64:1025–1035.

Furukawa, K., and S. Roth. 1985. Co-purification of galactosyltransferases from chick-embryo liver. *Biochem. J.* 227:573–582.

Goding, J. W. (1978). Conjugation of antibodies with fluorochromes: modifications to the standard methods. *J. Immunol. Methods.* 20:241–253.

Griffith, C. M., and M. J. Wiley. 1990. Sialoconjugates and development of the tail bud. *Development (Camb.).* 108:479–489.

Hamburger, V., and H. L. Hamilton. 1951. A series of normal stages in the development of the chick embryo. *J. Morphol.* 88:49–92.

Harvey, R. P., and D. A. Melton. 1988. Microinjection of synthetic Xhox-1A homeobox mRNA disrupts somite formation in developing Xenopus embryos. *Cell.* 53:687–697.

Hathaway, H. J., L. C. Romagnano, and B. S. Babiarz. 1989. Analysis of cell surface galactosyltransferase activity during mouse trophectodermal differentiation. *Dev. Biol.* 134:351–361.

Hathaway, H. J., R. B. Runyan, S. Khounlo, and B. D. Shur. 1991. Purification and characterization of avian β1,4 galactosyltransferase: comparison with the mammalian enzyme. *Glycobiology.* 1:211–221.

Hynes, R. O. 1987. Integrins: a family of cell surface receptors. *Cell.* 48: 549–554.

Kramer, H., R. L. Cagan, and S. L. Zipursky. 1991. Interaction of *bride of sevenless* membrane-bound ligand and the *sevenless* tyrosine-kinase receptor. *Nature (Lond.).* 352:207–212.

Kunemund, V., F. B. Jungalwala, G. Fischer, D. K. H. Chou, G. Keilhauer, and M. Schachner. 1988. The L2/HNK-1 carbohydrate of neural cell adhesion molecules is involved in cell interactions. *J. Cell Biol.* 106:213–223.

Larsen, E., T. Palabrica, S. Sajer, G. E. Gilbert, D. D. Wagner, B. C. Furie, and B. Furie. 1990. PADGEM-dependent adhesion of platelets to monocytes and neutrophils is mediated by a lineage-specific carbohydrate, LNF III (CD15). *Cell.* 63:467–474.

Lopez, L. C., E. M. Bayna, D. Litoff, N. L. Shaper, J. L. Shaper, and B. D. Shur. 1985. Receptor function of mouse sperm surface galactosyltransferase during fertilization. *J. Cell Biol.* 101:1501–1510.

Lowe, J. B., L. M. Stoolman, R. P. Nair, R. D. Larsen, T. L. Berhend, and R. M. Marks. 1990. ELAM-1–dependent cell adhesion to vascular endothelium determined by a transfected human fucosyltransferase cDNA. *Cell.* 63:475–484.

Martins-Green, M. 1988. Origin of the dorsal surface of the neural tube by progressive delamination of epidermal ectoderm and neuroepithelium: implications for neurulation and neural tube defects. *Development (Camb.).* 103: 687–706.

Martins-Green, M., and C. A. Erickson. 1987. Basal lamina is not a barrier to neural crest cell emigration: documentation by TEM and by immunofluorescent and immunogold labelling. *Development (Camb.).* 101:517–533.

Martins-Green, M. M., and K. T. Tokuyasu. 1988. A pre-embedding immunolabeling technique for basal lamina and extracellular matrix molecules. *J. Histochem. Cytochem.* 36:453–458.

Maxwell, G. D. 1976. Cell cycle changes during neural crest cell differentiation *in vitro*. *Dev. Biol.* 49:66–79.

Miller, D. J., N. L. Cross, M. Vazques-Levin, and B. D. Shur. 1992. The role of sperm galactosyltransferase in fertilization: presence and possible function in humans and other mammals. Serono Symposium VI. International Congress on Spermatology, Siena, Italy. 75:569–574.

Norenburg, J. L., and J. M. Barrett. 1987. Steedman's polyester wax embedment and de-embedment for combined light and scanning electron microscopy. *J. Electron Microsc. Technique.* 6:35–41.

Olson, D. J., J. L. Christian, and R. T. Moon. 1991. Effect of Wnt-1 and related proteins on gap junctional communication in Xenopus embryos. *Science (Wash. DC).* 252:1173–1176.

Perris, R., M. Paulsson, and M. Bronner-Fraser. 1989. Molecular mechanisms of avian neural crest cell migration on fibronectin and laminin. *Dev. Biol.* 136:222–238.

Placzek, M., M. Tessier-Lavigne, T. Yamada, T. Jessell, and J. Dodd. 1990. Mesodermal control of neural cell identity: floor plate induction by the notochord. *Science (Wash. DC).* 250:985–987.

Reddy, P., I. Caras, and M. Krieger. 1989. Glycosylation and the cell surface expression and stability of decay-accelerating factor, a glycophospholipid-anchored membrane protein. *J. Biol. Chem.* 264:17329–17336.

Romagnano, L., and B. Babiarz. 1990. The role of murine cell surface galactosyltransferase in trophoblast:laminin interactions *in vitro*. *Dev. Biol.* 141: 254–261.

Roth, J. M., J. Lentze, and E. G. Berger. 1985. Immunocytochemical demonstration of ecto-galactosyltransferase in absorptive intestinal cells. *J. Cell Biol.* 100:118–125.

Ruiz i Altaba, A., and D. A. Melton. 1989. Involvement of the Xenopus homeobox gene Xhox3 in pattern formation along the anterior-posterior axis. *Cell.* 57:317–326.

Runyan, R. B., G. D. Maxwell, and B. D. Shur. 1986. Evidence for a novel enzymatic mechanism of neural crest cell migration on extracellular glycoconjugate matrices. *J. Cell Biol.* 102:432–441.

Runyan, R. B., J. Versalovic, and B. D. Shur. 1988. Functionally distinct laminin receptors mediate cell adhesion and spreading: the requirement for surface galactosyltransferase in cell spreading. *J. Cell Biol.* 107:1863–1871.

Sainte-Marie, G. 1962. A paraffin embedding technique for studies employing immunofluorescence. *J. Histochem. Cytochem.* 10:250–256.

Schoenwolf, G. C., and J. L. Smith. 1990. Mechanisms of neurulation: traditional viewpoint and recent advances. *Development (Camb.).* 109:243–270.

Shur, B. D. 1977. Cell surface glycosyltransferases in gastrulating chick embryos. I: Temporally and spatially specific patterns of four endogenous glycosyltransferase activities. *Dev. Bio.* 58:23–39.

Shur, B. D. 1989. Glycoconjugates as mediators of cellular interactions during development. *Curr. Opinion Cell Biol.* 1:905–912.

Smith, C. A., and K. Brew. 1977. Isolation and characteristics of galactosyltransferase from Golgi membranes of lactating sheep mammary glands. *J. Biol. Chem.* 252:7294–7299.

Smith, J. L., and G. C. Schoenwolf. 1989. Notochordal induction of cell wedging in the chick neural plate and its role in neural tube formation. *J. Exp. Zool.* 250:49–62.

Stamenkovic, I., D. Sgroi, A. Aruffo, M. S. Sy, and T. Anderson. 1991. The B lymphocyte adhesion molecule CD22 interacts with leukocyte common antigen CD45RO on T cells and α2-6 sialyltransferase, CD75, on B cells. *Cell.* 66:1133–1144.

Takeichi, M. 1988. The cadherins: cell–cell adhesion molecules controlling animal morphogenesis. *Development (Camb.).* 102:639–655.

Tucker, G. C., J.-L. Duband, S. Dufour, and J. P. Thiery. 1988. Cell-adhesion and substrate-adhesion molecules: their instructive roles in neural crest cell migration. *Development (Camb.).* 103(Suppl.):82–94.

Vincent, M., and J. P. Thiery. 1984. A cell surface marker for neural crest and placodal cells: further evolution of the peripheral and central nervous system. *Dev. Biol.* 103:468–481.

Woo, H. J., L. M. Shaw, J. M. Messier, and A. M. Mercurio. 1990. The major non-integrin laminin binding protein of macrophages is identical to carbohydrate binding protein 35 (Mac-2). *J. Biol. Chem.* 265:7097–7099.